J. Fluid Mech. (1980), *vol.* 97, *part* 1, *pp.* 193–204
Printed in Great Britain

Theoretical calculations of turbulent bispectra

By JACKSON R. HERRING

National Center for Atmospheric Research,† Boulder, Colorado 80307

(Received 25 January 1979)

One-dimensional bispectra are computed from the statistical theory of turbulence (using the Test Field Model) and are compared with experiments. For an inertial range, we obtain $B(k_1, p_1) = \epsilon k^{-3} F(\theta)$, where B is the two-dimensional Fourier transform of $\langle u(\mathbf{x})\, u(\mathbf{x}+\hat{\imath}\xi_1)\, u(\mathbf{x}+\hat{\imath}\xi_2)\rangle$ with respect to (ξ_1, ξ_2), ϵ is the energy dissipation and $F(\theta)$ ($\theta = \tan^{-1}(k_1/p_1)$) is an angular distribution of order unity, which is compared to measurements of planetary boundary-layer turbulence. We also compare theory to wind tunnel data, as reported by Helland *et al.* (1978). Finally, we discuss to what extent the bispectra give insight into the dynamics of the flow.

1. Introduction

Lii, Rosenblatt & Van Atta (1976) and Helland, Lii & Rosenblatt (1978) have reported experimental measurements of bispectra for both wind-tunnel and planetary boundary turbulence. Such measurements contain important aspects of energy transfer that an analytic theory of turbulence should be able to explain. We recall in this connexion that the (velocity derivative) skewness is simply the integral of a bispectrum over a two-dimensional wavenumber domain (Lii *et al.* 1976), while the energy transfer function is just the three-dimensional bispectrum. However, as noted by Yeh & Van Atta (1973), a specification of the one-dimensional bispectrum is insufficient to derive the energy transfer function. Bispectra were originally proposed by Hasselman, Munk & MacDonald (1963) as a statistical means of describing nonlinear interacting ocean waves. McComas & Briscoe (1980) recently reported an extensive theoretical and experimental investigation of bispectra calculations for internal waves. A systematic account of their symmetry properties for isotropic turbulence has been presented by Craya (1958).

This paper reports theoretical results for the one-dimensional bispectrum using results from the direct-interaction approximation (DIA) (Kraichnan 1959), as well as the simpler test field model (TFM) (Kraichnan 1971). Results here are for self-similar decay at moderate Reynolds numbers and for an inertial range. At moderate Reynolds numbers, our theoretical results are in fair agreement with the experimental results cited above. At large Reynolds number (in the inertial subrange), the TFM method predicts the bispectrum to scale as wavenumber to the minus three, a result also obtained independently by Van Atta (1979). The distribution of the bispectra predicted by the theory agrees moderately well with that found experimentally. It

† The National Center for Atmospheric Research is sponsored by the National Science Foundation.

0022-1120/80/4396-8440 $02.00

indicates a strong non-local transfer (with large values near either wavenumber axis and a smooth distribution throughout the interior wavenumber domain).

Section 2 gives theoretical formulas derived from the DIA and TFM, as well as a sketch of how necessary integrations are performed. Results are presented in § 3 and compared to the experiments, while § 4 discusses what insights the bispectra can offer towards understanding the dynamics of turbulence.

2. Theory

2.1. *Kinematics*

We resolve a field of homogeneous turbulence of velocity $\mathbf{v}(\mathbf{x}, t)$ into Fourier components $\mathbf{u}(\mathbf{k}, t)$ by

$$\mathbf{v}(\mathbf{x}, t) = \sum_{\mathbf{k}} \exp(\mathbf{k}.\mathbf{x})\,\mathbf{u}(\mathbf{k}, t) \tag{1}$$

where, $\mathbf{k} = 2\pi(0, +1, +2, \ldots)/L$, and we suppose the flow to be periodic in a large cube of dimensions L^3. Next we define the triple moment Q by

$$Q_{ijn}(\mathbf{k}, \mathbf{p}, \mathbf{q}) = \langle u_i(\mathbf{k}, t)\, u_j(\mathbf{p}, t)\, u_n(\mathbf{q}, t)\rangle, \tag{2}$$

where the angular brackets represent the ensemble mean. A more experimentally assessable quantity simply related to Q is

$$B_{jmi}(k_1, p_1) = \left(\frac{L}{2\pi}\right)^6 \int_{-\infty}^{\infty} dk_2\, dk_3\, dp_2\, dp_3\, Q_{ijn}(\mathbf{k}, \mathbf{p}, \mathbf{q}), \quad \mathbf{q} = -\mathbf{p} - \mathbf{k}. \tag{3}$$

As noted by Lii *et al.* (1976), $\langle u(x)\, u(x+r_1)\, u(x+r_2)\rangle$ is the Fourier transform of the bispectrum $B_{111}(k_1, p_1)$ with respect to (k_1, p_1):

$$\langle u(x)\, u(x+r_1)\, u(x+r_2)\rangle = (2\pi)^{-2} \int dk_1\, dp_1\, B_{111}(k_1, p_1) \exp(i(k_1 r_1 + p_1 r_2)). \tag{4a}$$

It is also useful to define a bispectrum with respect to velocity derivatives B' such that

$$\langle (\partial u(x)/\partial x)\, (\partial u(x+r_1)/\partial r_1)\, (\partial u(x+r_2)/\partial r_2)\rangle = \int dk_1\, dp_1\, B'_{111}(k_1, p_1) \exp(i(k_1 r_1 + p_1 r_2)). \tag{4b}$$

From (4*a*), (4*b*) and (3),

$$B'(k_1, p_1) = ik_1 p_1 (k_1 + p_1)\, B(k_1, p_1). \tag{5}$$

Here omitted tensor subscripts are understood to be (111).

We take the turbulence to be isotropic so that the second-moment spectrum

$$U_{ij}(\mathbf{k}) = \langle u_i(\mathbf{k})\, u_j(-\mathbf{k})\rangle\, (L/2\pi)^3$$

is

$$U_{ij}(\mathbf{k}, t) = \tfrac{1}{2}(\delta_{ij} - k_i k_j/k^2)\, U(k, t) \equiv \tfrac{1}{2} P_{ij}(k)\, U(k, t). \tag{6}$$

Also needed are the two-time spectra $U(k, t, t') = \langle u(\mathbf{k}, t)\, u(-\mathbf{k}, t')\rangle (L/2\pi)^3$, for which (6) is also used, replacing $U(k, t)$ by $U(k, t, t')$ where needed without any further change in notation.

2.2. *Formulas from DIA and TFM*

The DIA expression for Q is

$$\begin{aligned} Q_{ijn}(\mathbf{k}, \mathbf{p}, \mathbf{q}) = (4i)^{-1} \delta(\mathbf{k} + \mathbf{p} + \mathbf{q}) \int_0^t ds\, \{ & (P_{im}(\mathbf{k})\, P_{mj}(\mathbf{p})\, P_{rn}(\mathbf{q})\, p_r + P_{ir}(\mathbf{k})\, P_{mj}(\mathbf{p})\, P_{rn}(\mathbf{q})\, q_m) \\ & \times G(k, t, s)\, U(p, t, s)\, U(q, t, s) + (\mathbf{k}, i \to \mathbf{p}, j; \mathbf{p}, j \to \mathbf{q}, n; \mathbf{q}, n \to \mathbf{k}, i) \\ & + (\mathbf{k}, i \to \mathbf{q}, n; \mathbf{p}, j \to \mathbf{k}, i; \mathbf{q}, n \to \mathbf{p}, j)\}. \end{aligned} \tag{7}$$

In (7), P_{ij} is given by (6) and $G_{ij}(k, t, s)$ measures the response in $u_i(\mathbf{k}, t)$ due to an

infinitesimal force field $f_j(\mathbf{k}, t')$ and $G_{ij} = P_{ij}(\mathbf{k})\, G$. Here and throughout this paper, summation on repeated vector indices is understood, unless explicitly exempted.

The TFM expression for Q is most easily described as an abridgment and modification of the ds-historical integral in (7). It replaces

$$\int_0^t ds\, G(k,t,s)\, U(p,t,s)\, U(q,t,s)$$

by

$$\int_0^t ds\, G^s(k,t,s)\, G^s(p,t,s)\, G^s(q,t,s)\, U(p,t)\, U(q,t), \tag{8}$$

where the G's are response functions of a test field and satisfy, for the compressive and solenoidal components,

$$(\partial/\partial t + \nu k^2 + \eta^{(c,s)}(k,t))\, G^{(c,s)}(k,t) = 0. \tag{9}$$

Expressions for the η's are contained in Kraichnan (1971) or in Herring & Kraichnan (1972); for brevity we shall not record them. We only note the inertial range form for the η's (Kraichnan 1971):

$$\eta(k) = c_s \epsilon^{\frac{1}{3}} k^{\frac{2}{3}}, \quad c_s = 0{\cdot}343 g^{\frac{4}{3}}, \tag{10a}$$

$$U(k) = 1{\cdot}342 g^{\frac{2}{3}} \quad (k^{-\frac{11}{3}}/2\pi). \tag{10b}$$

g is a scale factor, chosen to best match inertial range experiments ($g = 1{\cdot}5$). For self-similar decay, $\eta(k,t)$ is nearly independent of t so that (8) may be more conveniently approximated by

$$U(p,t)\, U(q,t)(1 - \exp(-\eta_{kpq} t))/\eta_{kpq}, \tag{11}$$

where

$$\eta_{kpq} \equiv \eta(n) + \eta(p) + \eta(q).$$

The DIA has a well-known failing of not properly distinguishing between large-scale convection and distortion. Consequently, its prediction for the inertial range is wrong ($k^{-\frac{3}{2}}$ instead of $k^{-\frac{5}{3}}$). This defect is remedied in the TFM by two changes: (1) a Markovianization, and (2) the introduction of relaxation time scales (reciprocals of the η's) which are invariant to large-scale convection. These changes effect a switch of the historical integral in (7) from Eulerian to Lagrangian character. The changes introduced in passing from the DIA to the TFM appear somewhat arbitrary, perhaps justifying the word model in the anagram. However, the theory models spectral detail [as contained in (7), (9), and (11)] rather than integral-scales of the motion, as in single-point or second-moment modelling. Thus, in general, no assumption of spectral self-similarity need be invoked but is rather a consequence of the theory. In the context of a perturbation theory, the TFM is a zeroth step in a formal self-consistent scheme (Kraichnan 1971). As in all such procedures, the zeroth order is at the disposal of the theorist.

Numerical studies of the TFM for both moderate and large Reynolds numbers suggest that it is a fairly accurate and economical procedure (Herring & Kraichnan 1972; Herring *et al.* 1974). This assessment includes comparisons with numerical simulations of Orszag & Patterson (1972) as well as with the data of Van Atta & Chen (1969).

2.3. *Reduction of integrals and numerical methods*

In the evaluation of $B_{111}(k_1, p_1)$, as given by (3), denote by $F(\mathbf{k}, \mathbf{p}, \mathbf{q})$ the terms on the right-hand side of (7) to the right of $\delta(\mathbf{k}+\mathbf{p}+\mathbf{q})$ (excluding the cyclic permutations) so that $Q_{111}(\mathbf{k}, \mathbf{p}, \mathbf{q})$ may be written as

$$Q_{111}(\mathbf{k}, \mathbf{p}, \mathbf{q}) = 4(i)^{-1}\delta(\mathbf{k}+\mathbf{p}+\mathbf{q})(F(\mathbf{k}, \mathbf{p}, \mathbf{q}) + F(\mathbf{p}, \mathbf{q}, \mathbf{k}) + F(\mathbf{q}, \mathbf{k}, \mathbf{p})). \tag{12}$$

The integrals in passing from (2) to (3) are conveniently done in cylindrical coordinates, with k_1 and p_1 taken as the axes of the cylinders. Inspection of (7) shows that the integrand for the cylindrical angular factors $(d\phi_k d\phi_p)$ depends only on $\psi \equiv (\phi_k - \phi_p)$ so that

$$\int d\phi_{\mathbf{k}} d\phi_p \ldots = 2\pi \int_0^{2\pi} d\psi \ldots .$$

To effect the remaining three integrals over the radial $(\mathbf{k}, \mathbf{p})$ dimensions (k_ρ and p_ρ) and ψ, transform to variables (k, p, q):

$$k^2 \equiv k_p^2 + k_1^2, \quad p^2 = p_p^2 + p_1^2,$$

and
$$q^2 = k^2 + p^2 + 2k_1 p_1 + 2(k^2 - k_1^2)^{\frac{1}{2}}(p^2 - p_1^2)^{\frac{1}{2}} \cos\psi.$$

Then for (3),

$$B(k_1, p_1) = -2\pi i \int_{|k_1|}^{\infty} k\,dk \int_{|p_1|}^{\infty} p\,dp \int_{q_-}^{q_+} q\,dq\, K(\mathbf{k}, \mathbf{p}, \mathbf{q}) \,(F(k, p, k_1, p_1) + F(p, q, k, p_1, q_1) + F(q, k, p, q_1, k_1)), \tag{13}$$

where
$$K(\mathbf{k}, \mathbf{p}, \mathbf{q}) = (4(k^2 - k_1^2)(p^2 - p_1^2) - (q^2 - k^2 - p^2 - 2k_1 p_1)^2)^{-\frac{1}{2}},$$

$$q_1 = -k_1 - p_1,$$

and
$$q_\pm^2 = k^2 + p^2 + 2k_1 p_1 \pm 2((k^2 - k_1^2)(p^2 - p_1^2))^{\frac{1}{2}}.$$

This method of decomposing integrals for B differs somewhat from that used by Yeh & Van Atta (1973) [see their equation (22)]. The present method is convenient here because the DIA form for Q as given by (7) is used. Yeh & Van Atta, on the other hand, decompose $B(\mathbf{k}, \mathbf{k}')$ $(\equiv Q(\mathbf{k}, \mathbf{p}, \mathbf{q})/\delta(\mathbf{k} + \mathbf{p} + \mathbf{q}))$ into its $(\mathbf{k}, \mathbf{k}')$-isotropic form, which involves the angle $\cos^{-1}(\mathbf{k}.\mathbf{k}'/kk') = \mu_k$, an angle that does not occur in (7). The methods are, of course, equivalent.

Note the symmetry condition,

$$B_{111}(k_1, p_1) = B_{111}(p_1, k_1), \tag{14a}$$

and the condition

$$B_{111}(0, p_1) = 0, \tag{14b}$$

which follows from the Fourier transform of (4a), if the ensemble mean flow is zero and if ensemble means are equivalent to spatial means.

Numerical evaluation of (13) is by Gaussian methods. First suppose that $U(k)$ decreases sufficiently rapidly so that any $(k, p, q) > k_{\max}$ contributions to (13) may be neglected with impunity. Then linearly map each of the three wavenumber regions $(k_1 \leqq k \leqq k_{\max})$, $(p_1 \leqq p \leqq k_{\max})$, $(q_- \leqq q \leqq \min(q_+, k_{\max}))$ into the interval $(-1, 1)$ and write the resulting integrals in the Gaussian form

$$\int_{-1}^{1} dx\,(1+x)^{\mu_1}(1-x)^{\mu_2} I(x) \cong \Sigma W(x_i)\, I(x_i) \tag{15}$$

(see, e.g., Stroud & Secrist 1966). Here $I(x)$, μ_1 and μ_2 are picked so that $I(x)$ is free from singularities. For the mapped-(k, p) integrals, $\mu_1 = \mu_2 = 0$. The values (μ_1, μ_2) for the mapped-q integration depend on whether the singularities of $K(\mathbf{k}, \mathbf{p}, \mathbf{q})$ are encountered in the mapped-q domain for fixed (k, p). If $k_{\max} \leqq q_+$, $\mu_1 = 0$, $\mu_2 = -\frac{1}{2}$; otherwise $\mu_1 = \mu_2 = -\frac{1}{2}$.

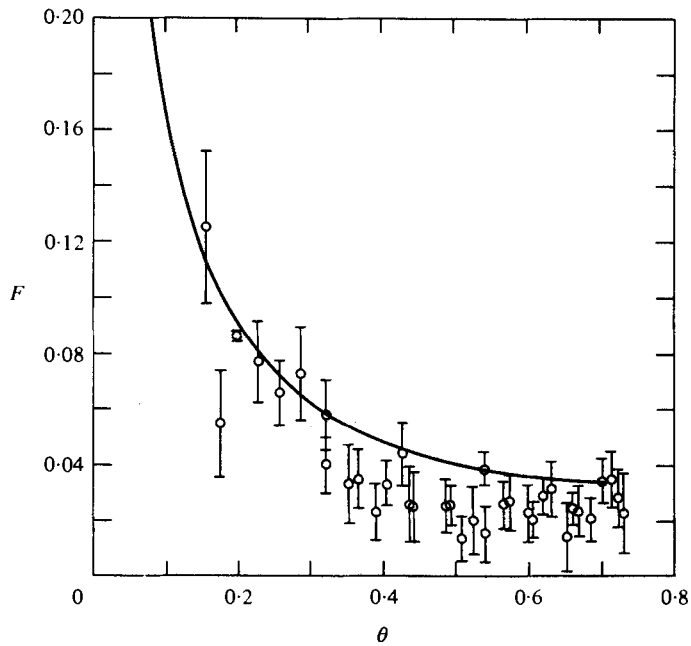

FIGURE 1. Inertial range one-dimensional bispectrum angular distribution [equation (16)] as a function of $\theta = \tan^{-1}(k_1^1/p_1)$. Points are data of Lii *et al.* (1976) as rescaled by Van Atta (1978). Solid line from TFM [equations (10*a*), (10*b*) and (13)].

3. Results

3.1. *Inertial range*

Inserting the inertial range forms for $\eta(k)$ and $U(k)$, as given by (10*a*) and (10*b*), into (13) results in

$$B_{111}(k_1, p_1) = \epsilon(k_1^2 + p_1^2)^{-\frac{3}{2}} F(\theta), \tag{16}$$

where $\theta = \tan^{-1}(p_1/k_1)$. ϵ is the dissipation of kinetic energy and the dimensionless function $F(\theta)$ is given in figure 1. The strong angular dependence of $F(\theta)$ on θ is indicative of the non-localness of the energy transfer mechanism. Similar observations have been made by Yeh & Van Atta (1973), Lii *et al.* (1976), and Helland *et al.* (1978) concerning the experimental data. Analytically, we have from (10*a*), (10*b*), and (7):

$$F(\theta) \to \theta^{-\frac{3}{2}} \quad \text{as} \quad \theta \to 0. \tag{17}$$

The points (and error bars) in figure 1 are the data of Lii *et al.* (1976), with a scaling worked out by Van Atta (1979) and independently by Helland (private communication). Agreement between theory and experiment appears satisfactory, with a deterioration in agreement as $\theta \to \frac{1}{4}\pi$, where the theoretical estimate exceeds experiment by $\sim 30\,\%$. We have no suggestion at present why theory should exceed the experiments. Perhaps the experimental values are smaller because some of them are near the dissipation range ($k/k_s \sim 0{\cdot}1$). It is interesting that no change occurs by adjusting the TFM scale factor g^2.

Other one-dimensional bispectra of possible interest are $B_{221}(k_1, p_1)$, $B_{122}(k_1, p_1)$, and $B_{212}(k_1, p_1)$. These are kinematically related by

$$B_{221}(k_1, p_1) = -B_{212}(p_1, -k_1 - p_1), \tag{18}$$

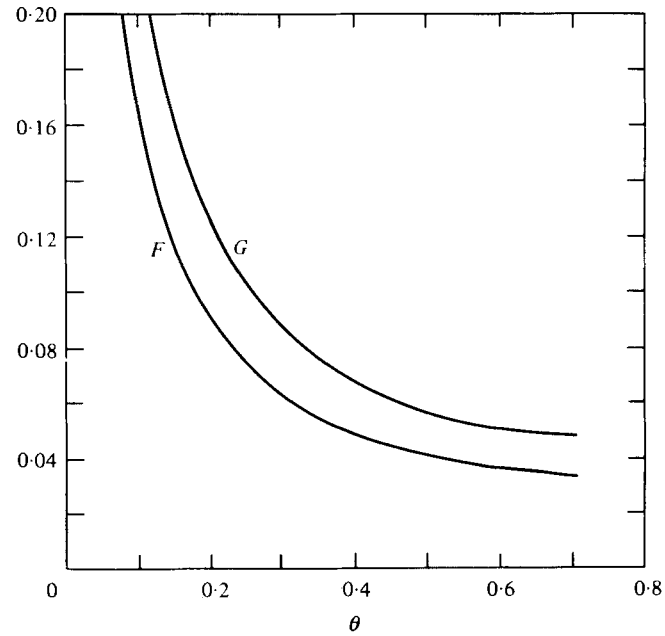

FIGURE 2. Angular distribution $G(\theta)$ for inertial range bispectrum $B_{221}(k_1, p_1)$ as a function of $\theta = \tan^{-1}(k_1/p_1)$. $F(\theta)$ according to TFM [equations (10a), (10b) and (13)].

and
$$B_{122}(k_1, p_1) = B_{221}(p_1, k_1), \tag{19}$$

irrespective of isotropy. For isotropic inertial-range turbulence, we may again characterize B_{221} by an equation like (16):

$$B_{212}(k_1, p_1) = (k_1^2 + p_1^2)^{-\frac{3}{2}} G(\theta) \tag{20}$$

and, similarly,

$$B_{221}(k_1, p_1) = (k_1^2 + p_1^2)^{-\frac{3}{2}} H(\theta). \tag{21}$$

From (18), we have

$$H(\theta) = -(1 + 2\sin\theta\cos\theta + \sin^2\theta)^{-\frac{3}{2}} G(-\tan(1 + \operatorname{cotan}\theta)). \tag{22}$$

Figure 2 gives the inertial range form of $G(\theta)$ for $-0 \leqslant \theta \leqslant \frac{1}{4}\pi$. $G(\theta)$ is slightly larger than $F(\theta)$ over the entire angular domain.

3.2. *Moderate-Reynolds-number results*

At moderate R_λ we compare results with the wind tunnel data of Helland *et al.* (1978). For these data, $R_\lambda \cong 40$ and a distinct inertial range does not exist. To make the comparison, we may set up an initial value problem whose initial R_λ is near 40 and whose shape evolves quickly (i.e. within a few eddy turnover times) into a near-self-similar profile, particularly at large k. One way of proceeding is to pick $E(k, 0)$ as

$$E(k, 0) = Ak\exp(-Bk). \tag{23}$$

Form (23) evolves into a completely self-similar shape with a constant R_λ, independent of time t. However, at large **t** (23) yields $E(t) = \int E(k, t)\,dk \sim t^{-1}$ apparently at variance with experiments, which appear more consistent with $E(t) \sim t^{-1.33}$ (Yeh & Van Atta 1973).

Alternatively, we could pick

$$E(k,0) = A'k^4 \exp(-B'k^2), \tag{24}$$

which at large R has been shown by Lesieur & Schertzer (1978) to evolve as $E(t) \sim t^{-1.39}$, with a $R_\lambda(t)$ which decreases with t. If (24) is used as initial data, the viscosity should be adjusted so that $R_\lambda(0) > 40$, and then theory and experiment should be compared for that t at which $R_\lambda(t) = 40$. $R_\lambda(0)$ should be picked sufficiently large that any initial transients are entirely damped out by the time $R_\lambda(t) = 40$. For the present runs, $R_\lambda(0) = 200$.

The two runs considered are: (1) $A = 0{\cdot}04$, $B = 0{\cdot}2$, $E(k,0)$ from (23), and $\nu = 0{\cdot}00147$; and (2) $A' = 0{\cdot}0004814$, $B' = 0{\cdot}04$, $E(k,0)$ from (24), and $\nu = 0{\cdot}00231$. Figure 3(*a*) compares the one-dimensional compensated energy spectrum,

$$\sim \tfrac{1}{2}k^{\frac{5}{3}} \int_k^\infty (1 - k^2/p^2) \frac{E(p)}{p} dp,$$

for runs (1) and (2). Little difference between (23) and (24) initial conditions is evident in the comparison, except at very small k. The one-dimensional dissipation spectrum $\phi(k)\, k^2$,

$$\phi(k) = \frac{1}{2} \int_k^\infty (1 - k^2/p^2)\, E(p)\, dp/p,$$

is compared in figure 3(*b*) to the data of Helland *et al.* (1978) (dashed line). Differences in $k^2\phi(k)$ between runs (1) and (2) are not detectable. The comparison with experiment is reasonably good. Figure 4 gives contours (for run 2) of the bispectra of velocity derivative [see equation (5)] scaled by the energy dissipation ϵ. The unit of wavenumber here is $k_s = (\epsilon/\nu^3)^{\frac{1}{4}}$.

We compare these theoretical calculations with the data of Helland *et al.* (1978) in figures 5(*a*, *b*). Figure 5(*a*) corresponds to our runs (1) or (2) above, while figure 5(*b*) is a similar perspective plot of their table 1 data. Here $B'(k_1, p_1)$ is again scaled by the energy dissipation and (k_1, p_1) by k_s. The comparison is reasonably good, but the theoretical estimates are significantly smaller than experiment near the peak of $B'(k_1, p_1)$. Such an underestimate of energy transfer at this wavenumber by the TFM relative to the data of Yeh & Van Atta (1973) has also been noted by Newman & Herring (1979). The above comparison is more clearly revealed by sectioning the reliefs of figure 5. Such sections are shown on figure 6 for several p_1 = constant slices. The experimental error bars are included in this comparison.

4. Conclusions

At large R_λ the theoretical estimates for $B(k_1, p_1)$ obtained by the TFM appear in reasonably good agreement with observations as presented by Helland *et al.* (1978) and by Van Atta (1978). How sensitive this result is to the underlying dynamics is yet to be discussed. For example, if we had used the DIA (with its wrong inertial range of $E(k) = c(E^{\frac{1}{2}}(t)\,\epsilon)^{\frac{1}{2}} k^{-\frac{3}{2}}$ and $\eta(k) \sim (E(t))^{\frac{1}{2}} k$), we would still find $B \sim k^{-3}$. The same remark holds for the eddy-damped Markovian quasi-normal theory (Orszag 1974). Hence, from the theoretical viewpoint the scaling law for B is somewhat insensitive

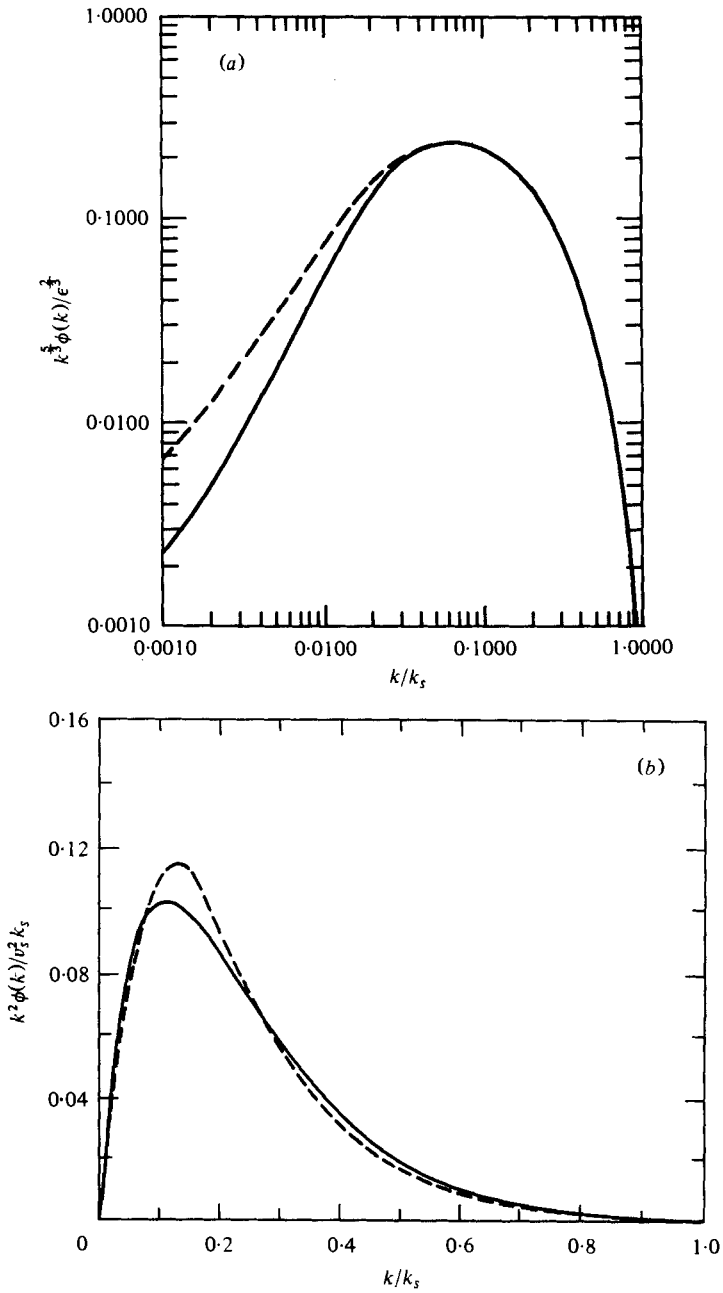

FIGURE 3. (*a*) One-dimensional compensated energy spectrum

$$k^{\frac{5}{3}}\epsilon^{-\frac{2}{3}}\phi(k) = \tfrac{1}{2}\epsilon^{-\frac{2}{3}}\int_k^\infty (1-k^2/p^2)\,E(p)\,dp/p)\,k^{\frac{5}{3}}$$

as given by: (1) TFM, $E(k, 0) = Ak \exp(-Bk)$, $\nu = 0{\cdot}0047$, $A = 0{\cdot}04$, $B = 0{\cdot}2$ (dashed line); (2) TFM, $E(k, 0) = A'k^4 \exp(-B'k)$, $\nu = 0{\cdot}00231$, $A' = 0{\cdot}0004814$, and $B' = 0{\cdot}04$ (solid line). (*b*) One-dimensional dissipation function $k^2\phi(k)$ as computed from runs (1) or (2). Comparison is made with data as given in figure 2 of Helland *et al.* (1978) (shown here as dashed line). The theoretical curves are the results of an initial value problem for which $R(t) = 50$. Kolmogorov scaling is used throughout.

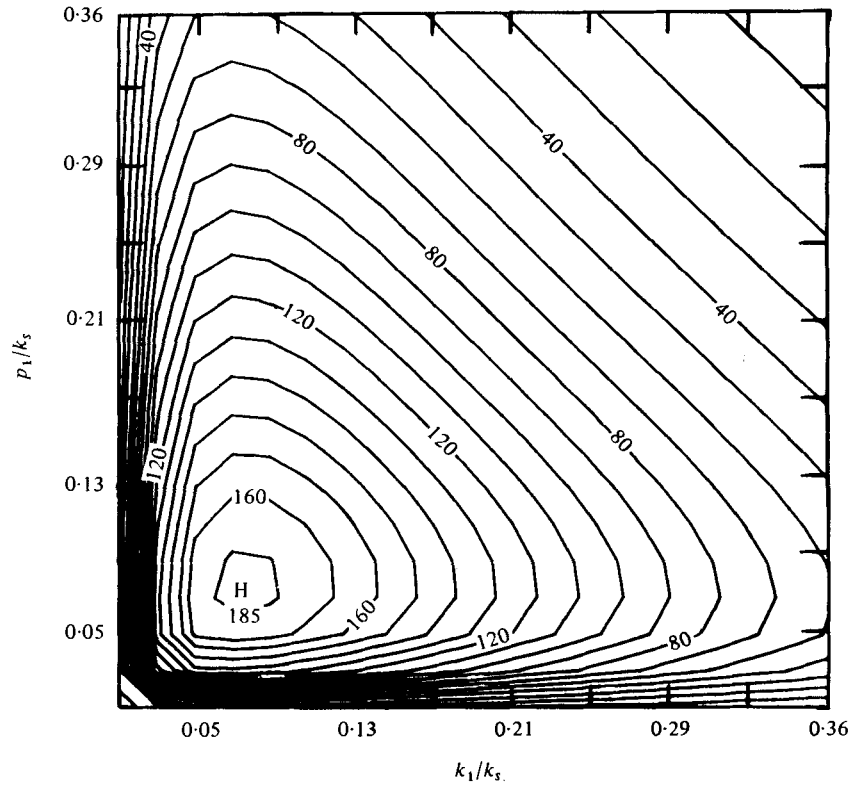

FIGURE 4. Contours of bispectrum $B'(k_1, p_1)$ [see equation (5)] for run (2). B' is in units of energy dissipation and wavenumber units are $(\epsilon/\nu^3)^{\frac{1}{4}}$.

to whether the time scales for the relaxation of triple moments are properly described in the theory used. The same remarks, of course, may also be made of the skewness. Thus, the *ansatz* that B depends only on ϵ and k does not isolate the Lagrangian dynamics of the energy transfer mechanism as does a similar statement about the energy spectrum.

At moderate R_λ, our results for $B'(k_1, p_1)$ are in qualitative agreement with experiments. Quantitatively, the TFM underestimates the energy transfer near the peak of $B'(k_1, p_1)$. One nice feature of the one-dimensional bispectrum not possessed by the energy transfer function is their near insensitivity to the energy spectrum at wavenumber k', if $k' < \min(k_1, p_1)$. An examination of (13) shows that $B(k_1, p_1)$ depends on $U(k')$ only through the dependence of $\eta(k)$ on $U(k')$. One may then expect that measurements of $B(k_1, p_1)$ for large (k_1, p_1) will not be very sensitive to the spectrum at small k, where the experimental flow is probably neither self-similar nor isotropic.

In closing, we mention that McComas & Briscoe (1980) reported recently an extensive investigation of bispectra of internal waves in the ocean. His theoretical procedure was weak wave interaction theory – identical to the (Markovian) quasi-normal approximation noted above. His comparison of theory and observation was somewhat hampered by a data record length. His conclusion 'that bispectra are too insensitive a technique for observing the nonlinear dynamics of the internal wave field' has, perhaps, a counterpart in hydrodynamic turbulence, where we have observed that the

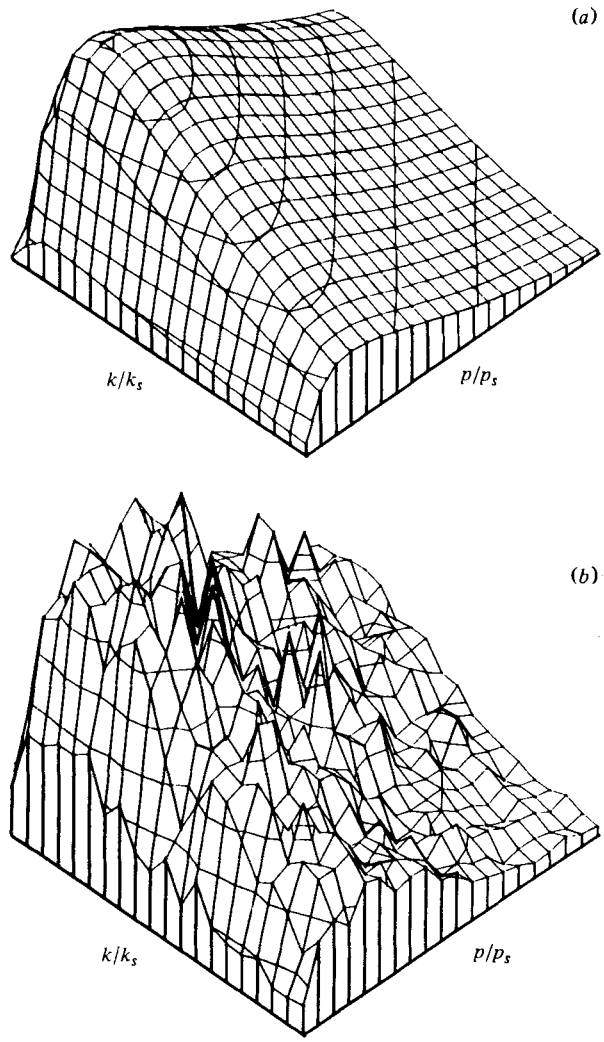

FIGURE 5. Perspective plots of $B'_{111}(k_1, p_1)$ (*a*) for run 2 and (*b*) the data of Helland *et al.* (1978). Units are the same as figure 4.

scaling law $B \sim k^{-3}$ is insensitive to the particular theory used. Only the angular distribution $F(\theta)$ [equation (16)] is sensitive to the dynamical time scales entering the theory. However, for hydrodynamical turbulence, the quality of inertial range data reported by Helland *et al.* (1978) and also the moderate R_λ data mentioned above are sufficient to assess the accuracy of theoretical procedures such as the DIA or TFM.

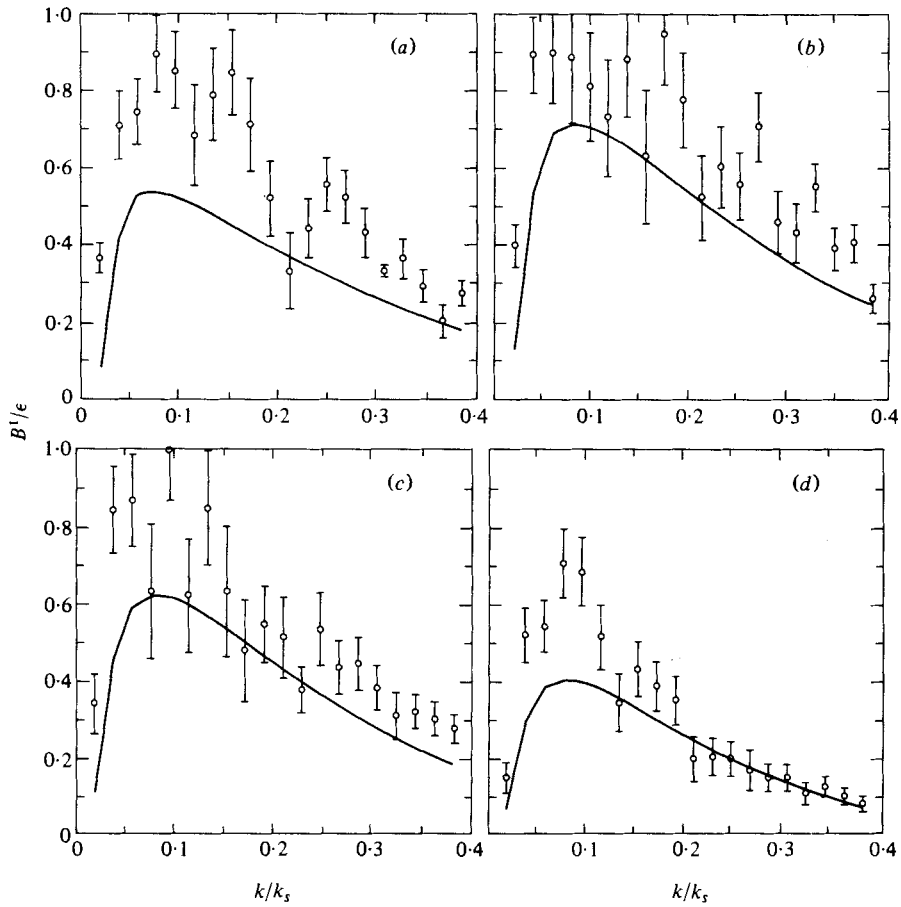

FIGURE 6. Sectioned plots of figure 5, i.e. $B'_{111}(k_1, p_1)$ for various p_1. Error bars on data as indicated by Helland *et al.* (1978). (*a*) $p_1/k_s = 0{\cdot}0383$; (*b*) $p_1/k_s = 0{\cdot}0767$; (*c*) $p_1/k_s = 0{\cdot}1534$; (*d*) $p_1/k_1 = 0{\cdot}2684$.

I thank Mr Larry Sapp for programming assistance in developing codes for the numerical integrations. I have benefited from several discussions with C. W. Van Atta, K. N. Helland, and M. Rosenblatt, and I am also grateful to them for constructive comments on the manuscript.

REFERENCES

CRAYA, A. 1958 Contribution a l'analyse de la turbulence associée a des vitesses moyennes. *Publ. Sci. Tech. Minist. Air (France)*.

HASSELMANN, K., MUNK, W. & MACDONALD, G. 1963 Bispectra of ocean waves. In *Time Series Analyses* (ed. M. Rosenblatt), pp. 125–139. Wiley.

HELLAND, K. N., LII, K. S. & ROSENBLATT, M. 1978 Bispectra of atmospheric and wind tunnel turbulence. In *Applications of Statistics* (ed. P. R. Krishniah), pp. 223–248. North Holland.

HERRING, J. R. & KRAICHNAN, R. H. 1972 Comparison of some approximations for isotropic turbulence. In *Statistical Models and Turbulence*, Lecture notes in physics, Vol. 12, pp. 148–194.

HERRING, J. R., ORSZAG, S. A., KRAICHNAN, R. H. & FOX, D. G. 1974 Decay of two-dimensional homogeneous turbulence. *J. Fluid Mech.* **66**, 417–444.

KRAICHNAN, R. H. 1959 The structure of isotropic turbulence at very high Reynolds numbers. *J. Fluid Mech.* **5**, 497–543.

KRAICHNAN, R. H. 1971 An almost-Markovian Galilean-invariant turbulence model. *J. Fluid Mech.* **47**, 513–524.

LESIEUR, M. & SCHERTZER, D. 1978 Dynamic des gros Tourbillons et Décroissance de L'énergie Cinétique en Turbulence Tridimensionelle Isotype à Grand Nombre de Reynolds. *J. Méc.* **17**, 609–646.

LII, T. T., ROSENBLATT, M. & VAN ATTA, C. W. 1976 Bispectral measurements in turbulence. *J. Fluid Mech.* **77**, 45–62.

MCCOMAS, C. H. & BRISCOE, M. G. 1980 A note on the bispectra of internal waves. *J. Fluid Mech.* **97**, 205–213.

NEWMAN, G. R. & HERRING, J. R. 1979 A test field model study of a passive scalar in isotropic turbulence. *J. Fluid Mech.* **94**, 163–194.

ORSZAG, S. A. 1974 *Statistical Theory of Turbulence: Les Houches Summer School on Physics.* Gordon & Breach.

ORSZAG, S. A. & PATTERSON, G. S. 1972 Numerical simulation of three-dimensional homogeneous isotropic turbulence. *Phys. Rev. Lett.* **28**, 76–79.

STROUD, A. H. & SECRIST, D. 1966 *Gaussian Quadrature Formulas.* Englewood Cliffs, N.J.: Prentice-Hall.

VAN ATTA, C. W. & CHEN, W. Y. 1969 Measurements of spectral energy transfer in grid turbulence. *J. Fluid Mech.* **38**, 743–763.

VAN ATTA, C. W. 1979 Inertial range bispectra in turbulence. *Phys. Fluids.* **22**, 1440–1442.

YEH, T. T. & VAN ATTA, C. W. 1973 Spectral transfer of scalar and velocity fields in heated-grid turbulence. *J. Fluid Mech.* **58**, 233–261.